Applied Energy 156 (2015) 767–775

Contents lists available at ScienceDirect

Applied Energy

journal homepage: www.elsevier.com/locate/apenergy

Influences of activation agent impregnated sewage sludge pyrolysis on emission characteristics of volatile combustion and De-NOx performance of activated char

Hui Chen, Dezhen Chen *, Liu Hong

Thermal and Environmental Engineering Institute, School of Mechanical Engineering, Tongji University, 1239 Siping Road, Shanghai 200092, China

HIGHLIGHTS

- Emission characteristics of volatile combustion from SS pyrolysis were investigated with and without activation agent impregnation.
- SO_2, NO, N_2O and HCl are main emissions from SS pyrolysis volatile combustion.
- SO_2 emission can be avoided when KOH and $ZnCl_2$ is impregnated into SS before pyrolysis.
- Char produced from KOH-impregnated SS pyrolysis shows the best De-NOx efficiency.

ARTICLE INFO

Article history:
Received 18 February 2015
Received in revised form 25 May 2015
Accepted 28 May 2015
Available online 13 June 2015

Keywords:
Sewage sludge
Pyrolysis
Volatile combustion
Emission
Activated char
De-NOx

ABSTRACT

In this study, KOH and $ZnCl_2$ were impregnated into sewage sludge as activation agents to produce activated sludge char in the pyrolysis step for the De-NOx process. The emission characteristics of volatile combustion from the pyrolysis of raw sewage sludge (SS-Raw), sewage sludge spiked with KOH (SS-KOH), and sewage sludge spiked with $ZnCl_2$ (SS-$ZnCl_2$) were investigated. In addition, the De-NOx effects and the characteristics of the prepared chars, including specific surface areas, pore distributions, functional groups, were explored. The exploration results showed that the pollutants generated during the volatile combustion process could be divided into primary pollutants (SO_2, NO, N_2O, and HCl) and minor pollutants (CO, NH_3, and HCN). Under the conditions of oxygen-rich combustion, SO_2 and NOx emissions from SS-KOH were 0% and 113.2% of those from SS-Raw respectively. SS-$ZnCl_2$ exhibited the similar SO_2 and NOx emissions to those of SS-KOH. However, SS-$ZnCl_2$ released considerable HCl during the pyrolysis process, thus limiting its application. Sludge char from SS-KOH (SC-KOH) also exhibited the best De-NOx performance compared to the chars from SS-Raw and SS-$ZnCl_2$ and the De-NOx efficiency was 56% higher than that of sludge char from SS-Raw (SC-Raw). Therefore, with KOH-impregnated SS, activated sludge char can be produced via one pyrolysis step and used in the De-NOx process.

1. Introduction

Sewage sludge (SS) is a by-product of wastewater treatment and composed of organic compounds, macronutrients, a wide range of micronutrients, non-essential trace metals, organic micro pollutants, and microorganisms [1] and its final disposal is one of the most troublesome environmental issues. Available SS disposal technologies include incineration for energy recovery and land application for nutrient conservation. However, when the common lower heat value (LHV) of the SS in China is relatively low, for example lower than 10,000 kJ/kg, the goal of recovering energy from SS incineration cannot be achieved. Moreover, the SS contaminated by heavy metals are not suitable for land application. Recently, SS gasification has been developed to produce high quality fuel gas [2,3], but its practicability still depends on the high LHV of SS. Alternative thermal treatment is pyrolysis, a thermal degradation of material in an oxygen-deficient atmosphere or in the absence of air [4]. In pyrolysis, SS undergoes similar volume reduction process compared to incineration or gasification, but pyrolysis has many advantages. For example, heavy metal vaporization is inhibited due to the decreased operation temperature and the leaching of heavy metals from the carbonaceous residue (char) is greatly abated [5], even they are actively impregnated [6]. Moreover, the target products from pyrolysis are miscellaneous. For example, biochar [7], adsorbents [8–10], or catalysts [11–13]

* Corresponding author. Tel.: +86 21 65985009; fax: +86 21 65982786.
E-mail address: chendezhen@tongji.edu.cn (D. Chen).

http://dx.doi.org/10.1016/j.apenergy.2015.05.098
0306-2619/

are the potential valuable products derived from char. The combustible volatile (oil and gas) generated in the pyrolysis process maybe burned online to supply energy to the pyrolysis reactor [4,14,15], thus reducing or avoiding commercial fuel consumption and achieving an energy-saving disposal. In practice, energy supply via direct combustion of volatile is crucial for a sustainable carbonization process of biomass, including SS [16]. For such a sustainable carbonization process, emission from the volatile combustion is the only pollutant source in the whole disposal.

The char from SS pyrolysis can be used as fuel [17–19]. However, due to its low LHV, to recover the char as adsorbent for gaseous emission abatement [10,20] or catalysts for De-NOx [12] is more valuable commercially and safer environmentally. However, the pore development of the SS chars is highly dependent on various factors during the pyrolysis and activation processes. In most cases, activation agents are inevitable for promoting the adsorption or catalytic effects [10].

Chars from SS pyrolysis post-treated with activating agents such as salt activation agent ($ZnCl_2$), acid activation agent (H_3PO_4 or H_2SO_4), and alkali activation agent (KOH or NaOH) were reported to promote the better adsorption or catalytic effects [10,21]. To reach good activation, those activation agents are usually adopted as post-treatment chemicals after char production [15,17,20]. However, the post-treatment of char is a complicated process, which is usually associated with huge energy consumption (physical activation) or water pollution (chemical activation). Chiang et al. [21,22] added activating agents into raw sewage sludge materials and found that proper $ZnCl_2$-immersed biosludge produced mesoporous adsorbents. They also indicated that the pyrolysis of $ZnCl_2$-immersed sewage sludge resulted in highly chlorinated volatile organic compounds (VOC) emission. However, VOC emitted in pyrolysis can be destroyed during the volatile combustion process, whereas the emission characteristics of pyrolysis volatile combustion for sewage sludge pre-spiked with various activating agents were seldom reported. To choose the proper activation agent, both these emissions and char quality should be integrally considered.

In this study, to simplify the activated char production and prevent emissions in the overall process, including the char production process and the utilization process, raw sewage sludge, sewage sludge impregnated with KOH, and sewage sludge impregnated with $ZnCl_2$ underwent pyrolysis to obtain the activated char for the De-NOx process. The paper focused on the emissions caused by their pyrolysis volatile combustion. Based on the information on the De-NOx performance and the emission characteristics, we recommended the proper activation agent to produce activated char for De-NOx processes in one pyrolysis step.

2. Materials and methods

2.1. Materials

Sewage sludge samples were obtained from a sewage treatment plant in Shanghai, China, where municipal wastewater is treated according to the standard activated sludge method. All the chemicals used including $N_2H_4{\cdot}H_2O$, $ZnCl_2$, KOH, $Fe(NO_3)_3$, and $Mn(NO_3)_2$ were of analytical grade (Sinopharm Chemical Reagent, China).

The raw sewage sludge had an original total solid content of 20 ± 2 wt.%. Raw sewage sludge was dried before analysis. An elemental analysis of the samples was performed using a Vario EL III elemental analyzer (Elementar Analysensysteme GmbH, Germany). The proximate analysis was carried out according to the GB/T 28731-2012 standard [23]. Ash content was determined at 550 °C and the volatile matter was determined at 900 °C. All analyses were performed in triplicates. The results are presented as mean ± standard deviation (SD), as shown in Table 1.

2.2. SS sample preparation

SS samples with or without activation agent impregnated were prepared for char production via the pyrolysis step. Those sludge samples are summarized in Table 2. KOH and $ZnCl_2$ were used as activation agents and $Fe(NO_3)_3$ & $Mn(NO_3)_2$ were used to enhance the catalytic effects. The activation agents adopted in Table 2 and the dosages of SS-$ZnCl_2$ and SS-KOH were following the reports by Peng et al. [24] and Cha et al. [12], respectively.

To prepare SS-$ZnCl_2$, the solutions of $ZnCl_2$, $Fe(NO_3)_3$, and $Mn(NO_3)_2$ were blended for 2 h with the raw SS sample using an agitator to yield a good mixture with metal incorporation. According to the method suggested by Peng et al. [24], the $ZnCl_2$-to-sludge mass ratio was 1:1 on a dry basis, and the Zn^{2+}-to- (Fe^{2+}+Mn^{2+}) mole ratio was 1:0.5. In SS-KOH preparation, the KOH-to-sludge mass ratio was 1:1 based on the dry mass for chemical activation. Then, the raw SS sample and KOH- and $ZnCl_2$-impregnated SS samples were dried for more than 24 h in an oven at 105 °C to obtain SS-Raw, SS-KOH, and SS-$ZnCl_2$.

2.3. Pyrolysis of SS samples for char production

Fig. 1 shows the schematic diagram of the pyrolysis system for the production of activated char samples. Instead of post treatment of the char with activation agents after pyrolysis adopted in the previous study by Cha et al. [12], here all the activation agents are contained in the prepared SS samples before the pyrolysis step. The experimental apparatus consisted of a pyrolysis reactor, a combustion chamber for the pyrolysis volatile, and an online flue gas analysis system. The pyrolysis reactor was heated up by a series of electrical heating elements. In the pyrolysis reactor, the SS samples were kept in an inert atmosphere provided by N_2 flushing, as shown in Fig. 2.

To produce the activated char for De-NOx process, 100 g of each prepared SS sample, including SS-Raw, SS-KOH and SS-$ZnCl_2$ was packed into the pyrolysis reactor, respectively. Then, the pyrolysis reactor was heated up at a rate of 25 °C min^{-1} under N_2 flow of 60 ml min^{-1}. The pyrolysis temperature was set to be 650 °C and the retention time was 30 min.

The obtained char samples were then washed with distilled water to remove the soluble K^+, Zn^{2+}, Fe^{3+}, and Mn^{2+}. The washed sampled were then dried in an oven at 110 °C for 24 h and then sieved through a sieve (150–200 mesh). The obtained sewage sludge char samples were hereafter referred to as SC-Raw, SC-KOH, and SC-$ZnCl_2$. The samples were stored in a refrigerator until utilization.

2.4. Volatile combustion and emission analysis

To save energy, the volatile was recommended to be burnt online to supply the energy for the pyrolysis reaction (Fig. 1). The volatile (including oil and gas) generated from pyrolysis reactor was injected into a combustion chamber immediately before cooling (Fig. 2).

To ensure the complete combustion, the volatile was transferred into a combustion chamber (Fig. 2). In the combustion chamber, the volatile was mixed with pure O_2 flow at a flow rate to ensure an oxygen-rich combustion environment (with excess air coefficient greater than 2). An ignition device was adopted to ignite the volatile–O_2 mixture in the chamber, and the temperature in the chamber is maintained within 700–800 °C with the aid of the electric heating device.

The flue gas generated from the combustion chamber was cooled down in an ice-bath, and an acidic gas such as HCl was absorbed in the wash bottle train with water. Then, the insoluble O_2, CO, NO, N_2O, NO_2, SO_2, and HCN were analyzed online using

Table 1
Characteristics of sewage sludge.

Proximate analysis (dry basis)					Ultimate analysis/% (dry basis)			
A/%	V/%	FC/wt.%	Q_{net}/kJ kg^{-1}		[C]	[H]	[O]	[N]
27.3 ± 0.6	63.6 ± 1.2	9.1 ± 0.2	15.65 ± 0.52		37.5 ± 0.8	5.9 ± 0.1	19.9 ± 0.1	5.4 ± 0.1
Metal content analysis/mg g^{-1}								
Al	As	B	Ba	Cr	Cu	Fe	K	Li
7.732 ± 0.101	1.180 ± 0.0002	6.583 ± 0.087	3.819 ± 0.067	0.030 ± 0.022	0.927 ± 0.002	10.229 ± 0.476	10.063 ± 0.239	1.587 ± 0.234
Mg	Mn	Ni	P	Pb	Se	Sr	V	Zn
3.653 ± 0.169	0.278 ± 0.002	0.025 ± 0.0002	12.214 ± 0.577	0.0560 ± 0.0007	0.030 ± 0.0002	0.082 ± 0.004	0.006 ± 0.002	2.957 ± 0.104

(A: ash content; V: volatile content; FC: fixed carbon)

Table 2
Nomenclatures of prepared sludge samples.

Samples	Activation agents	Supported metals
SS-Raw	/	/
SS-KOH	KOH	/
SS-$ZnCl_2$	$ZnCl_2$	$Fe(NO_3)_3$, $Mn(NO_3)_2$

a Gasmet DX4000 (Gasmet Technologies OY, Finland) fourier transform infrared spectrometer connected to the outlet of the washing bottle train in the ice-bath and the data were recorded using a computer.

2.5. Activity evaluation of the sludge chars

2.5.1. Characterization

The physical characteristics of the obtained sludge chars, including the specific surface area, the total pore volume distribution, and the pore diameter, were measured via N_2 adsorption using an ASAP 2020 micropore analyser (Micromeritics Co., USA) at −196.15 °C in liquid N_2. The specific surface area was calculated according to the Brunauer–Emmett–Teller (BET method). The Barrett–Joyner–Halenda (BJH) method was used to determine the pore size distribution.

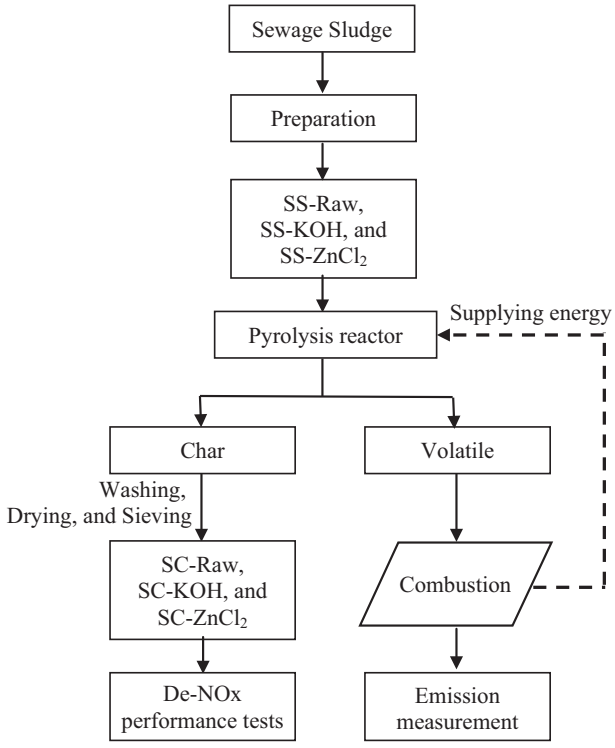

Fig. 1. Schematic diagram of producing activated char for De-NOx process.

In the spectroscopic characterization of the obtained sludge chars, a fixed amount of sample was thoroughly mixed with KBr (FTIR grade, from Merck) according to the ratio 1:100 (w/w). Subsequently, the mixture was made into pellets before analysis. FTIR analyses were performed using an EQUINOXSS/HYPER, Bruker Vertex 70 spectrometer (Bruker Co., Germany) in the region of 4000–400 cm^{-1} at a resolution of 0.5 cm^{-1} to identify the functional groups (—COOH, —OH, and —COO, C═O) formed on the char surface.

2.5.2. De-NOx experiments

To evaluate the effect of sludge char on the De-NOx process, we adopted a De-NOx reactor consisting of a vertical furnace with a sludge char layer in the middle as an absorbent or catalyst (Fig. 3). The inlet gas consisted of NO (500 ppm), O_2 (5–8 vol.%), and balanced N_2. Three grams of char sample was used in each test and the char sample weight/flow rate of flue gas (W/F ratio) was 1.67 g·(L min^{-1})$^{-1}$, which corresponded to a space velocity inside the reactor of 10,727 h^{-1}. The relatively high space velocity inside the reactor was adopted to enhance the char saturation with NO and shorten the reaction duration. When checking the function of the chars as an absorbent, no reducing agent was added and the inlet and outlet NOx concentrations were analyzed to define the difference. When evaluating the catalytic effect of these chars, hydrazine hydrate solution was used as the reducing agent [25]. Hydrazine hydrate solution has been reported to be more active at lower temperatures [26]. The De-NOx temperature in the reactor was set to be 250 °C and the high temperatures above 300 °C were avoided to prevent char oxidation as well as CO formation. The De-NOx effects were recorded with time and the data were reported as integral means during 10 min together with their upper and lower deviations. The De-NOx experiments were repeated to ensure the difference between the parallel integral means less than 5%.

The NOx removal efficiency η was calculated as:

$$\eta = \frac{[NO_x]_{in} - [NO_x]_{out}}{[NO_x]_{in}} \times 100\% \quad (R1)$$

where $[NO_x]_{in}$ and $[NO_x]_{out}$ are the inlet and outlet NOx concentrations (vol.%) of the De-NOx reactor.

3. Results and discussion

3.1. Emission behaviors from volatile combustion

To ensure the complete combustion, pure O_2 was supplied to the combustion zone of the volatiles to maintain an oxygen-rich atmosphere. Oxidation products in the exhaust were CO_2, SO_2, H_2O and NOx; and unburned components such as H_2, CH_4 or

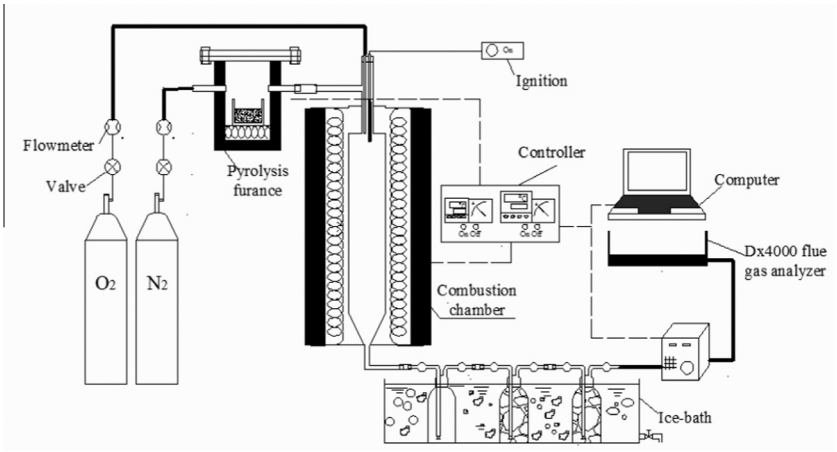

Fig. 2. Schematic diagram of the experimental system for the char production and volatile combustion.

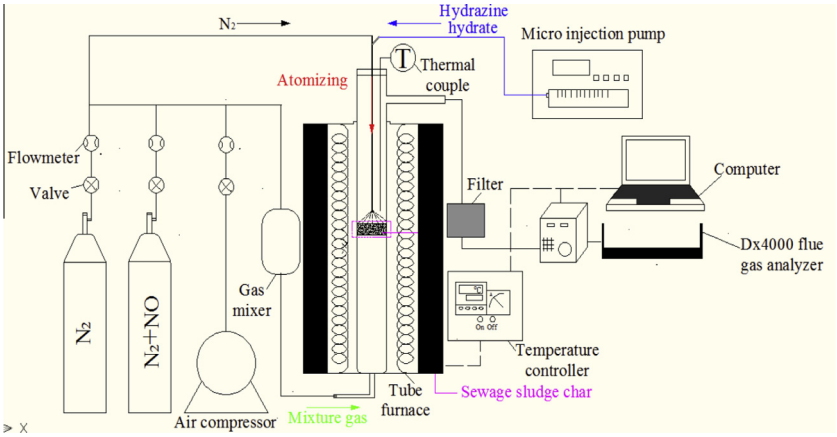

Fig. 3. Schematic diagram of the char testing system for De-NOx.

C_xH_y were not detected. The results indicate the complete combustion of pyrolysis volatiles in the combustion chamber [27].

3.1.1. Average emission from volatile combustion

Fig. 4 shows the pollutant emission performances of volatile combustion when the three SS samples undergo pyrolysis. Although the Gasmet DX4000 analyzer can measure other pollutants such as C_2H_5Cl, HNCO, and SO_3, only those species shown in Fig. 4 are detected. It can be seen that the pollutants include CO, SO_2, NO, NO_2, N_2O, NH_3, HCN and HCl. Among them, SO_2, NO, N_2O and HCl were the main pollutants especially when the volatile from SS-Raw was burned. The emissions such as CO, NH_3, and HCN also appeared due to poor blending in the combustion chamber, but their concentrations were very low.

It should be noted that the data in Fig. 4 were calibrated to mL per gram of activated char. For the three types of SS samples, the emission patterns of all the pollutants except SO_2 and HCl are similar (Fig. 4). Under the same production of activated char, SS-Raw released the most SO_2 and SS-$ZnCl_2$ released the most HCl due to evaporation of Cl in the sludge impregnated with $ZnCl_2$, as reported by Chiang et al. [21]. SO_2 release was largely inhibited in both SS-KOH and SS-$ZnCl_2$. SO_2 emissions in SS-KOH and SS-$ZnCl_2$ were respectively only 0% and 0.9% of that from SS-Raw, suggesting that both KOH and $ZnCl_2$ effectively captured sulfur.

It has been reported that the species containing carbon in the volatile from sewage sludge pyrolysis are primarily aromatic compounds containing oxygen, such as phenols, alcohols, fluorines,

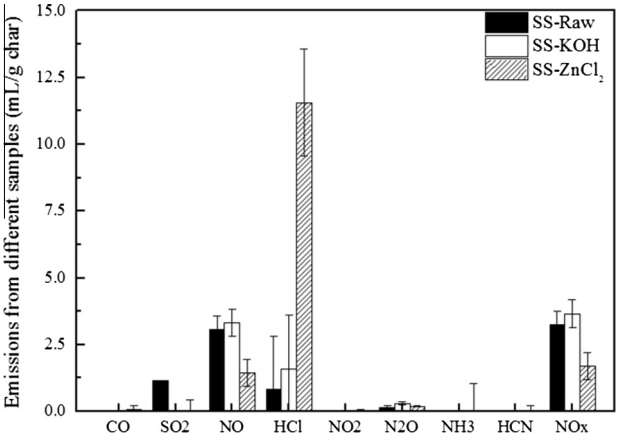

Fig. 4. Emissions from the combustion of pyrolysis volatiles (in mL g^{-1} char, integral values with their upper and lower deviations).

aldehydes, and ketones [28,29], which are then oxidized to form CO_2 in the oxygen-rich combustion chamber, as given by R2:

$$C_iH_jO_k + O_2 \rightarrow CO_2 + CO + H_2O \quad (R2)$$

Some volatiles contain sulphur compounds, such as H_2S, COS, SO_2, and CS_2. Among these sulphur compounds, H_2S represents the main component [30]. After oxygen-rich combustion, most of

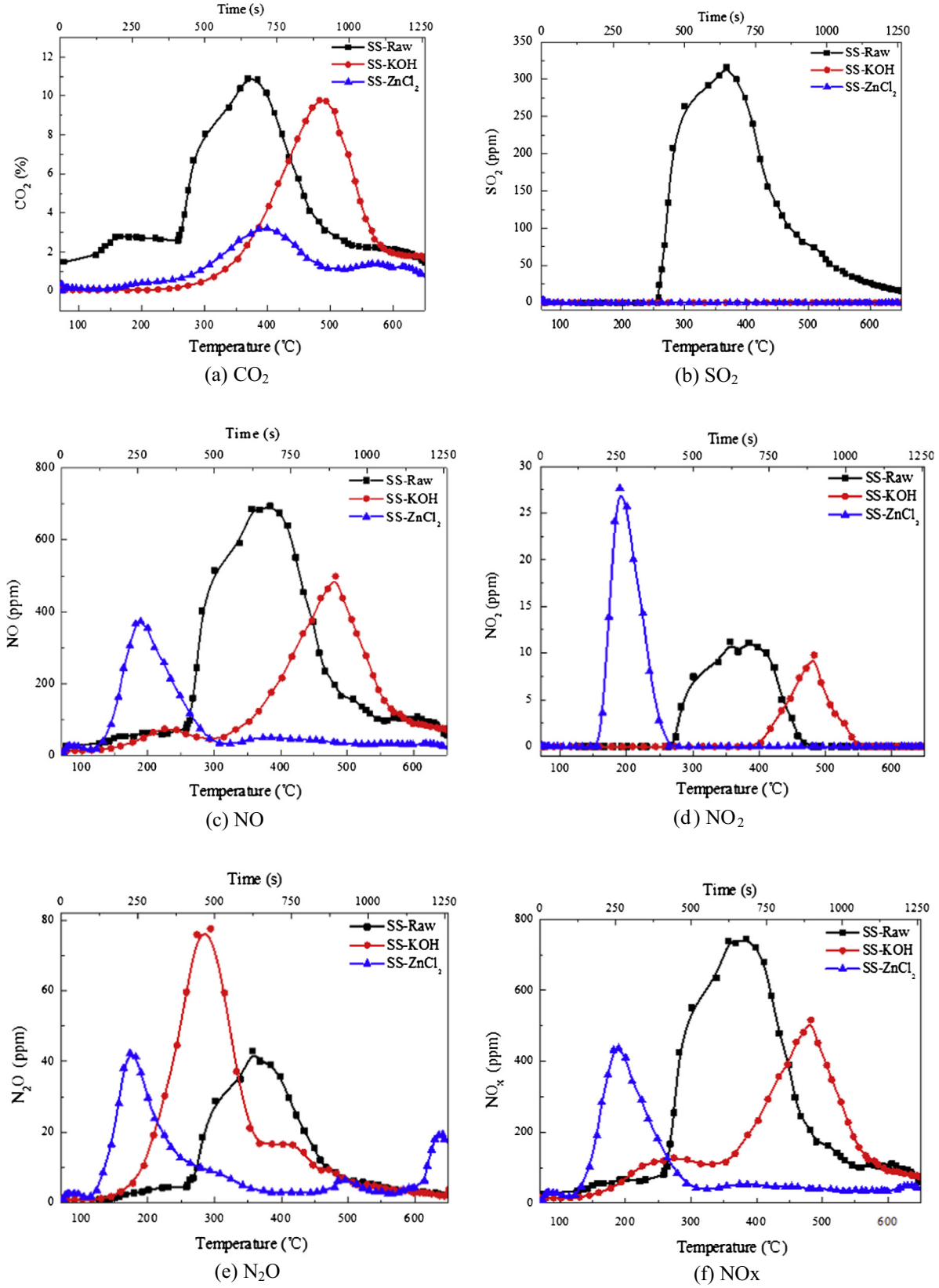

Fig. 5. Emission profiles of different pollutants after volatile combustion as a function of pyrolysis temperature (calibrated to O_2 = 11%).

Table 3
Physical properties of different sludge chars.

Samples	BET/$m^2\ g^{-1}$	Total pore volume/$cm^3\ g^{-1}$	Pore size/nm
SC-Raw	93.69 ± 0.01	0.067 ± 0.001	2.85 ± 0.10
SC-KOH	180.41 ± 0.01	0.173 ± 0.001	3.84 ± 0.10
SC-$ZnCl_2$	278.98 ± 0.01	0.358 ± 0.001	5.13 ± 0.10

these sulphur compounds are oxidized to form SO_2, as given by R3, which explains the emission of SO_2 for the case of SS-Raw in Fig. 4,

$$H_2S + O_2 \rightarrow SO_2 + H_2O \quad (R3)$$

Pyrolysis gases contain large amounts of nitrogen compounds such as NH_3, HCN, and HCNO [30]. However, after combustion, these nitrogen compounds were decomposed or oxidized and little compounds were left in the flue gas, as shown in Fig. 4. Oxidation of these nitrogen compounds can be expressed as:

$$NH_3 + O_2 \rightarrow NO_2 + NO + H_2O \quad (R4)$$

$$HCN + O_2 \rightarrow NO_x + CO_2 + CO + H_2O \quad (R5)$$

$$HCNO + O_2 \rightarrow NO_x + CO_2 + H_2O \quad (R6)$$

Fig. 4 shows that the pollutant NOx is primarily found in SS-Raw and SS-KOH. The phenomenon can be explained by the higher concentrations of nitrogen compounds in their volatiles. For the same amount of each sludge sample (SS-Raw, SS-KOH, and SS-$ZnCl_2$), the mass of activated char obtained after washing and drying was decreased according to the following sequence: SS-KOH > SS-$ZnCl_2$ > SS-Raw. This indicates that a larger amount of SS-KOH is required for producing a certain amount of activated char, which increases the likelihood of NOx generation during pyrolysis and volatile combustion. As a result, NOx emissions from SS-KOH and SS-$ZnCl_2$ were 113.2% and 52.4% of that from SS-Raw.

Of course the emission characteristics of volatile combustion are heavily dependent on the combustion parameters, such as temperature [31] and oxygen blending mode [32]. However, under a certain condition, the generation of SO_2 and NOx from combustion is directly related to the contents of N and S and their compound species in the fuel. As oxygen-rich combustion is provided here with the same excess air coefficient at almost the same temperature, the differences in emissions maybe caused by the different N-compounds, hydrocarbons and their concentrations in volatile, which is the consequence of activation agent addition in SS samples.

3.1.2. Emission behaviors from volatile combustion versus pyrolysis temperature

Fig. 5 shows the emissions of CO_2, SO_2, NO/NOx, and NO_2/N_2O from the three sewage sludge samples as a function of pyrolysis temperature or time.

Fig. 5(a) shows that the content of CO_2 released from SS-Raw is low below 250 °C, suggesting that hydrocarbons are not essentially released below 250 °C. When the temperature reached 250 °C, CO_2 emission began to rise sharply, reached a maximum level of 11%, and then began to decrease after 380 °C. The CO_2 emission curve shows an extensive release of hydrocarbons in the temperature range of 250–480 °C during SS-Raw pyrolysis. For SS-KOH, the corresponding temperature range was shifted to 370–560 °C, and the maximum level of CO_2 was lower than that of SS-Raw. For SS-$ZnCl_2$, the level of CO_2 was highly reduced and the maximum concentration is less than 4% (v/v), indicating that the release of hydrocarbons during the SS-$ZnCl_2$ pyrolysis process was largely inhibited.

Fig. 5(b) shows that for SS-Raw, S-compounds are released at pyrolysis temperatures above 250 °C, reaching its peak content at approximately 370 °C, which is the same temperature at which the CO_2 content peaks. Then, SO_2 gradually decreases, suggesting that S-compounds are emitted at the same temperature to hydrocarbons. No SO_2 was released due to the pyrolysis of SS-KOH and SS-$ZnCl_2$. Several salts, such as ZnS or K_2S, might be formed during the blending and pyrolysis processes and trapped sulphur when KOH and $ZnCl_2$ were impregnated into the raw sludge. SO_2 emission behaviors shown in Fig. 5(b) suggest that KOH or $ZnCl_2$ impregnation pyrolysis is beneficial to the prevention of SO_2 release compared to char activation afterward [12].

Fig. 5(c)–(f) shows that nitrogen compounds are also released at the same temperatures as hydrocarbons during the SS-Raw pyrolysis process and that the release behaviors of NO_x, including NO, N_2O, and NO_2, exhibit the same trend as CO_2. The release behaviors of NO_x from SS-$ZnCl_2$ and KOH exhibited different features compared to SS-Raw. SS-$ZnCl_2$ was associated with the earlier appearance of NO_x, suggesting that nitrate salts, such as $Fe(NO_3)_3$ and $Mn(NO_3)_2$, spiked together with $ZnCl_2$, were decomposed below 200 °C. However, at temperatures higher than 200 °C, NOx formation was inhibited. Although spiking with KOH delayed the formation of NO and NO_2, it enhanced the formation of N_2O. SS-KOH corresponded to NO emissions at higher temperatures, which might be caused by the altered structure of N-containing compounds in the sludge [33]. In addition, more N_2O was emitted because the added KOH raised the pH of the sludge and various intermediate products, such as NH_2OH and NO_2^--N, were released into the volatile to form N_2O [34]. However, N_2O formation can be prevented by increasing the combustion temperature during the combustion [35]. The curves of NOx release as a function of the pyrolysis temperature were almost equivalent to those of NO as NO represented the major portion of NOx (Fig. 5(f)). In general, $ZnCl_2$ impregnation resulted in a reduction in the total NOx formation due to combustion of pyrolysis volatiles, but the high HCl emission limits its application.

3.2. De-NOx performances of the chars

3.2.1. Physical properties of the chars

Table 3 provides the specific areas and pore characteristics of the sludge char (SC) samples. Fig. 6 shows the pore size distribution of different sewage sludge char samples calculated according to the BJH method. The specific areas and total pore volume increased considerably when the sewage sludge was activated by spiking with $ZnCl_2$ and KOH. However, the specific surface area and total pore volume of SC-KOH were lower than those of SC-$ZnCl_2$ (Fig. 6 and Table 3). Li et al. [10] argued that the type of activation agent directly affected the micropore structure, specific

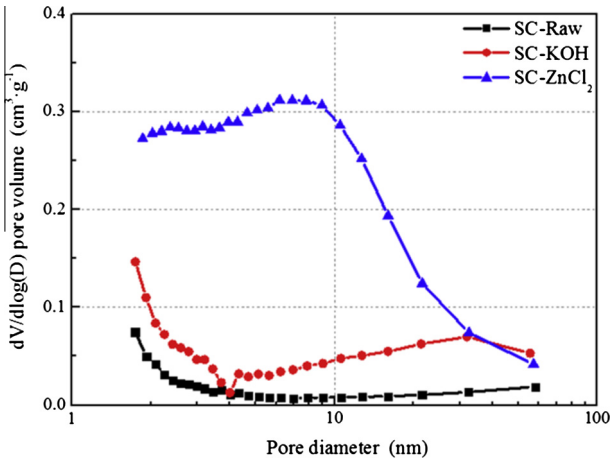

Fig. 6. BJH pore size distribution of different sludge chars.

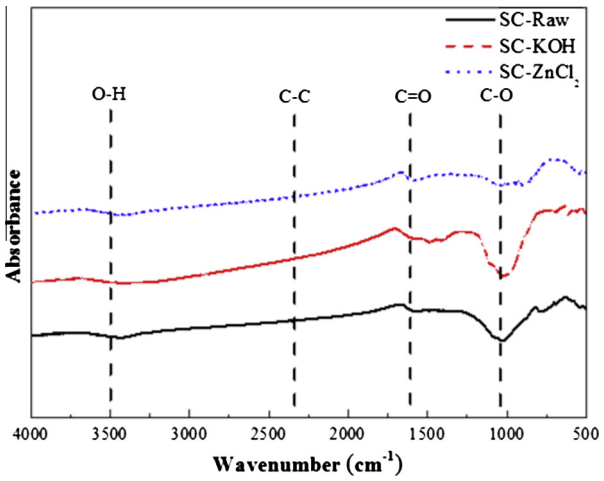

Fig. 7. FTIR spectra of the SCs prepared under different conditions.

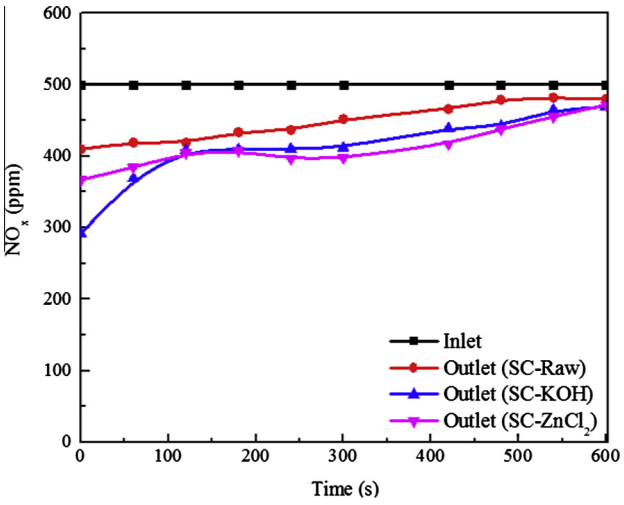

Fig. 9. NOx breakthrough curves at 250 °C.

surface area, and total pore volume of the SC samples and found that the specific surface area and total pore volume of the sludge activated chars with a salt activating agent ($ZnCl_2$) were larger than that of chars with an acid activating agent (H_3PO_4 or H_2SO_4) and that chars with an alkali activating agent (KOH or NaOH) exhibited the smallest specific surface area and total pore volume. However, in the paper, the specific surface and total pore volume of SC-KOH is almost two times of that of the SC-Raw.

3.2.2. FT-IR analysis

To identify the functional groups formed in SC samples, the FT-IR spectra of the three chars were obtained (Fig. 7). The peaks of all of the SC samples within the wavelength range of 3650–3200 cm^{-1} indicated O-H stretching of hydroxyl groups [13]. However, a significant alkynes C≡C vibration peak [36] did not appear at 2332 cm^{-1}. The peaks at 1612 cm^{-1} were prescribed to the C=O stretching [12], whereas the C—O stretching vibration peak appeared within the wavelength range of 1200–1100 cm^{-1} [37]. The peak intensities of C—O and C=O of three samples were increased according to the following sequence: $SC\text{-}ZnCl_2$ < SC-Raw < SC-KOH, indicating that oxygen functional groups, such as C=O and C—O, were more easily developed on the char surface due to impregnating the sludge with KOH.

3.2.3. De-NOx performances

The De-NOx performances of the obtained sludge char were investigated (Fig. 8). The De-NOx reducing agent used here was not a conventional reducing agent such as ammonia or urea, but a more active reducing agent, namely, hydrazine hydrate solution for its activity at low temperatures [25]. The different SC samples were used as either absorbents or catalysts and the De-NOx temperature was controlled at 250 °C.

Fig. 8 shows the De-NOx efficiency of the flue gas under different oxygen concentrations. The first bar row in Fig. 8(a) and (b) shows the adsorption effect of SC samples on NOx without spraying reductant, and the breakthrough curves of different sludge chars (Fig. 9) show that SC-KOH and $SC\text{-}ZnCl_2$ have the better De-NOx adsorption effect than SC-Raw. As the hydrazine hydrate solution was sprayed into the reaction region, the NOx removal efficiencies increased. As shown in Fig. 8, the middle bars indicate the general De-NOx efficiency under the combination of adsorption and catalysis and the right bars indicate the subtracted results of the left and middle bars. SC-KOH exhibited a slightly larger NOx absorption capability and a better catalytic effect among the three sludge char samples, followed by $SC\text{-}ZnCl_2$. Compared to SC-Raw, both SC-KOH and $SC\text{-}ZnCl_2$ were activated as an adsorbent or a catalyst. However, $SC\text{-}ZnCl_2$ exhibited a larger specific surface area and total pore volume than SC-KOH (Table 3), suggesting a negative correlation between the specific surface area and De-NOx efficiency. Ahmed et al. [38] reported that the chemical properties of activated carbons, such as surface oxides and mineral matters, were more important factors for De-NOx performance than the physical properties, including specific surface area and pore structure. Therefore, it was deduced that the functional groups

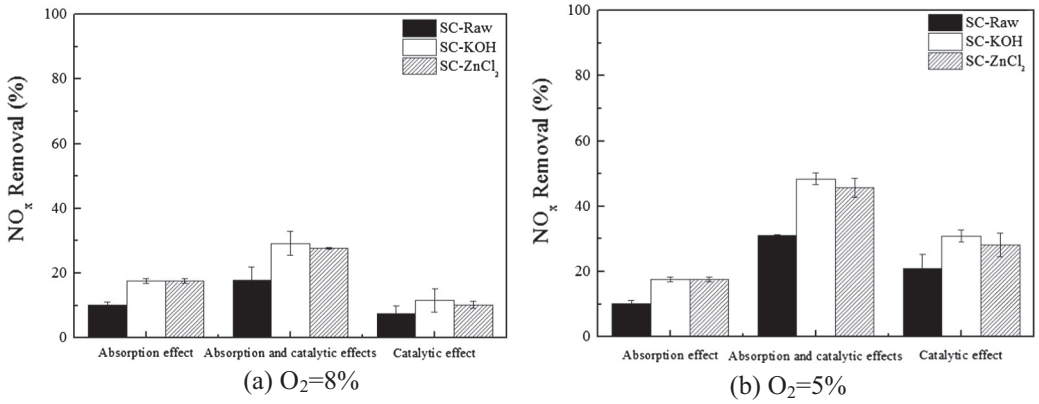

Fig. 8. SC used for De-NOx under different O_2 concentrations.

developed on the surface of SC-KOH (Fig. 7) led to a slightly higher NO_x removal efficiency compared to SC-$ZnCl_2$. Generally compared to SC-raw, SC-KOH exhibited a catalytic De-NOx efficiency of 56% higher than SC-raw, but the valid life span of the sludge char should be investigated further.

Comparing Fig. 8(a) with (b), it can be seen that the NOx removal efficiency increases with the decrease in the oxygen concentration. If the oxygen level was high, the NH_2 concentrations generated from hydrazine hydrate decreased, resulting in a lower NOx removal, which could be explained according to R7–R9 [39].

$$N_2H_4(+M) \rightarrow N_2H_2 + N_2H_2(+M) \quad (R7)$$

$$N_2H_2 + NO \rightarrow N_2 + H_2O \quad (R8)$$

$$N_2H_2 + NO \rightarrow N_2O + NH_2 \quad (R9)$$

Considering the pollutants emitted from the volatile combustion during the preparation of the sewage sludge chars, SC-KOH is a feasible candidate catalyst. HCl emitted during SC-$ZnCl_2$ production process can be an obstacle for its utilization as HCl is highly corrosive to heat transmission surface. Compared to char production from SS-Raw followed by activating treatment, activation agent-impregnated SS pyrolysis is recommended, and KOH maybe a proper activation agent. The total emissions are reduced and the post-treatment energy can be saved in this activated char production approach.

4. Conclusions

In order to produce activated sewage sludge (SS) char for De-NOx process and avoid extensive post-treatment of the char through the combination with pyrolysis step, the activation agent-impregnated SS pyrolysis was investigated to grasp the emission characteristics of volatile combustion during the pyrolysis and the activation effects of $ZnCl_2$ and KOH were checked by investigating their De-NOx performance. Experimental results showed that the main pollutants from the volatile combustion were SO_2, NO, N_2O, and HCl. KOH and $ZnCl_2$ impregnation SS pyrolysis is effective in inhibiting the evaporation of S-containing compounds from SS, resulting in zero SO_2 emissions during volatile combustion. Both SC-KOH and SC-$ZnCl_2$ are activated chars for the De-NOx process compared to SC-Raw. SC-KOH exhibited the best De-NOx performance, but NOx emission slightly increased during its production. HCl emission from SS-$ZnCl_2$ pyrolysis was the main drawback associated with SC-$ZnCl_2$ application. The De-NOx efficiency of SC-KOH is 56% higher than that of SC-raw. Considering the emission characteristics of volatile combustion and De-NOx efficiency, SC-KOH is a competitive option for the production of activated char. The study also indicated that activation agent impregnation SS pyrolysis could be an environmentally friendly and energy-saving approach for the production of activated char with SS.

Acknowledgment

This research was supported by the China National 863 Plan project (Grant No. 2012AA063504).

References

[1] Wei Y, Liu Y. Effects of sewage sludge compost application on crops and cropland in a 3-year field study. Chemosphere 2005;59:1257–65.
[2] Leng LJ, Yuan XZ, Chen XH, Huang HJ, Wang H, Li H, et al. Characterization of liquefaction bio-oil from sewage sludge and its solubilisation in diesel microemulsion. Energy 2015;82:218–28.
[3] Werle S, Dudziak M. Gaseous fuels production from dried sewage sludge via air gasification. Waste Manage Res 2014;32:601–7.
[4] Gascó Blanco CG, Guerrero F, Méndez Lázaro AM. The influence of organic matter on sewage sludge pyrolysis. J Anal Appl Pyrol 2005;74:413–20.
[5] Hwang IH, Ouchi Y, Matsuto T. Characteristics of leachate from pyrolysis residue of sewage sludge. Chemosphere 2007;68:1913–9.
[6] Xue XY, Wang H, Song XD, Zhou GM, Chen DZ. Leaching characteristics of chars from five wastes pyrolysis process. In: Proceedings of the fourteenth international waste management and landfill symposium, Sardinia, Italy; 2013.
[7] Agrafioti E, Bouras G, Kalderis D, Diamadopoulos E. Biochar production by sewage sludge pyrolysis. J Anal Appl Pyrol 2013;101:72–8.
[8] Gómez-Pacheco CV, Rivera-Utrilla J, Sánchez-Polo M, LópezPeñalve JJ. Optimization of the preparation process of biological sludge adsorbents for application in water treatment. J Hazard Mater 2012;217–218:76–84.
[9] Lin QH, Cheng H, Chen GY. Preparation and characterization of carbonaceous adsorbents from sewage sludge using a pilot-scale microwave heating equipment. J Anal Appl Pyrol 2012;93:113–9.
[10] Li F, Yan B, Zhang YP, Zhang LH, Lei T. Effect of activator on the structure and desulphurization efficiency of sludge-activated carbon. Environ Technol 2014;35:2575–81.
[11] Jo YB, Cha JS, Ko JH, Shin MS, Park SH, Jeon JK, et al. NH_3 catalytic reduction (SCR) of nitrogen oxides (NOx) over activated sewage sludge char. Korean J Chem Eng 2011;28:106–13.
[12] Cha JS, Choi JC, Ko JH, Park YK, Park SH, Jeong KE, et al. The low-temperature SCR of NO over rice straw and sewage sludge derived char. Chem Eng J 2010;156:321–7.
[13] Ko JH, Kwak YH, Yoo KS, Jeon JK, Park SH, Park YK. Selective catalytic reduction of NOx using RDF char and municipal solid waste char based catalyst. J Mater Cycles Waste Manag 2011;13:173–9.
[14] Shen L, Zhang DK. Low-temperature pyrolysis of sewage sludge and putrescible garbage for fuel oil production. Fuel 2005;84:809–15.
[15] Domínguez A, Menéndez JA, Inguanzo M, Pís JJ. Production of bio-fuels by high temperature pyrolysis of sewage sludge using conventional and microwave heating. Bioresour Technol 2006;97:1185–93.
[16] Mura E, Debono O, Vilot A, Paviet F. Pyrolysis of biomass in a semi-industrial scale reactor: study of the fuel-nitrogen oxidation during combustion of volatiles. Biomass Bioenergy 2013;59:187–94.
[17] Chun YN, Kim SC, Yoshikawa K. Pyrolysis gasification of dried sewage sludge in a combined screw and rotary kiln gasifier. Appl Energy 2011;88:1105–12.
[18] Hwang IH, Matsuto T, Tanaka N, Sasaki Y, Tanaami K. Characterization of char derived from various types of solid wastes from the standpoint of fuel recovery and pretreatment before landfilling. Waste Manage 2007;27:1155–66.
[19] Zhao PT, Ge SF, Yoshikawa K. An orthogonal experimental study on solid fuel production from sewage sludge by employing steam explosion. Appl Energy 2013;113:1213–21.
[20] Chen HF, Namioka T, Yoshikawa K. Characteristics of tar, NOx precursors and their absorption performance with different scrubbing solvents during the pyrolysis of sewage sludge. Appl Energy 2011;88:5032–41.
[21] Chiang HL, Lin KH, Chiu HH. Exhaust characteristics during the pyrolysis of $ZnCl_2$ immersed biosludge. J Hazard Mater 2012;229:233–44.
[22] Chiang HL, Lin KH, Chiu HH. Emission factor of exhaust gas constituents during the pyrolysis of zinc chloride immersed biosolid. Environ Sci Pollut Res 2013;20:5718–89.
[23] AQSIQ and SAC. Proximate Analysis of Solid Biofuels. General administration of quality supervision, inspection and quarantine of the People's Republic of China and Standardization administration of the People's Republic of China. (GB/T 28731-2012). Gov Print Office, Beijing; 2012 [in Chinese].
[24] Peng L, Li CT, Li CX, Zhai YB, Huang XG, Lu P, et al. Preparation of catalyst for denitrification using raw sludge and metal oxide. Chin J Chem Eng 2008;2:522–6 [in Chinese].
[25] Hong L, Yin LJ, Chen DZ, Wang D. Proposal and verification of a kinetic mechanism model for NOx removal with hydrazine hydrate. AIChE J 2015;61:904–12.
[26] Lee JB, Kin SD. NOx reduction by hydrazine in a pilot-scale reactor. Chem Eng J 1998;69:99–104.
[27] Wijayanta AT, Alam MS, Nakaso K, Fukai J, Shimizu M. Optimized combustion of biomass volatiles by varying O_2 and CO_2 levels: a numerical simulation using a highly detailed soot formation reaction mechanism. Bioresour Technol 2012;10:645–51.
[28] Luo R, Wu S, Lv GJ, Yang Q. Energy and resource utilization of deinking sludge pyrolysis. Appl Energy 2012;90:46–50.
[29] Petersen I, Werther J. Experimental investigation and modelling of gasification of sewage sludge in the circulating fluidized bed. Chem Eng Process 2005;44:717–36.
[30] Tan LL, Li CZ. Formation of NOx and SOx precursors during the pyrolysis of coal and biomass. Part II: Effects of experimental conditions on the yields of NOx and SOx precursors from the pyrolysis of a Victorian brown coal. Fuel 2000;79:1891–7.
[31] Buhre BJP, Elliott LK, Sheng CD, Gupta RP, Wall TF. Oxy-fuel combustion technology for coal-fired power generation. Prog Energy Combust 2005;31:283–307.
[32] Hu S, Naito S, Kobayashi N, Hasatani M. CO_2, NOx and SO_2 emission from the combustion of coal with high oxygen concentration gases. Fuel 2000;79:1925–32.
[33] Wang ZH, Zhang JY, Zhao YC, Zheng CG. Release features of NOx precursors during the pyrolysis and gasification of sewage sludge. J Huazhong Univ of Sci & Tech: Natural Sci Ed 2011;39:98–101.

[34] Wrage N, Velthof GL, Van Benusichem ML, et al. Role of nitrifier denitrification in the production of nitrous oxide. Soil Biol Biochem 2001;33:1723–32.
[35] Roy B, Chen LG, Bhattacharya S. Nitrogen oxides, sulphur Trioxide, and mercury emissions during oxyfuel fluidized bed combustion of Victorian brown coal. Environ Sci Technol 2014;48:14844–50.
[36] Lua AC, Yang T. Effect of activation temperature on the textural and chemical properties of potassium hydroxide activated carbon prepared from pistachio-nut shell. J Colloid Interface Sci 2004;274:594–601.
[37] Olivares-Marín M, Fernández-González C, Macías-García A, Gómez-Serrano V. Preparation of activated carbon from cherry by chemical activation with $ZnCl_2$. Appl Surf Sci 2006;252:5967–71.
[38] Ahmed SN, Stencel JM, Derbyshire FJ, Baldwin RM. Activated carbons for the removal of nitric oxide. Fuel ProcessTechnol 1993;34:123–36.
[39] Caton JA, Xia ZY. The selective Non-catalytic Removal (SNCR) of nitric oxides from engine exhaust streams: comparison of three processes. J Eng Gas Turb Power 2004;126:234–9.